# A Single-Mode Rheological Model for Steady Flows of Polymer Melts

**Jia Yang,[1] Ji-Zhao Liang,[1] Kejian Wang[2]**

[1]*School of Mechanical and Automobile Engineering, South China University of Technology, Guangzhou 510640, People's Republic of China*
[2]*Institute of Plastics Machinery and Engineering, Beijing University of Chemical Technology, Beijing 100029, People's Republic of China*

Received 9 April 2011; accepted 4 November 2011
DOI 10.1002/app.36453
Published online 1 February 2012 in Wiley Online Library (wileyonlinelibrary.com).

**ABSTRACT:** The steady shear viscosity ($\eta_s$), the steady first normal stress coefficient ($\Psi_1$), the steady second normal stress coefficient ($\Psi_2$), and extensional viscosity ($\eta_e$) are four important parameters for polymer melts during polymer processing. In this article, we propose a stress and rate-dependent function to describe creation and destruction of polymer junctions. Moreover, we also introduce a movement expression to describe nonaffine movement of network junctions. Based on network theory, a nonaffine single-mode rheological model is presented for the steady flow of polymeric melts, and the equations of $\eta_s$, $\Psi_1$, $\Psi_2$, and $\eta_e$ are derived from the model accordingly. Furthermore the dependences of $\eta_s$ and $\eta_e$ on model parameters are discussed for the model. Without a complex statistical simulation, the single-mode model with four parameters yields good quantitative predictions of the steady shear and extensional flows for two low density polyethylene melts reported from previous literature in very wide range of deformation rates. © 2012 Wiley Periodicals, Inc. J Appl Polym Sci 125: 3107–3114, 2012

**Key words:** polymer; single-mode; rheology; steady flow

## INTRODUCTION

Rheological properties of polymeric melts are important during polymer processing, which can significantly affect the processing technology and final properties of products. Hence, many rheological models have been derived to describe the rheological properties of polymeric materials in several decades.[1–4] One of the important models is a single-mode network model, the single-mode model only needs a set of parameters to control and predict shear and extensional properties simultaneously,[5] the parameters in single-mode model are easy to be determined, and it is convenient for implementation in polymer processing and finite element simulation. In general, the relationship between steady shear viscosity and shear rate accords to a law equation at high shear rate, and the exponent is between 0 and 1, however, the exponent derived from a basic network single-mode model is $-2$.[1] On the other hand, based on the experimental facts polymer melts also cannot be extended indefinitely, for some polymer melts the steady extensional viscosity increases with increasing extensional rate initially, reaches a maximum and then decreases with further increase of the extensional rate. However at a finite extensional rate steady extensional viscosity tends to infinity for some single-mode models.[1,5] Moreover, predicted steady first and second normal stress coefficients also deviate from the experimental results. Therefore, many researchers proposed different ways to improve the predictive ability of single-mode network model.

A common and effective approach is that the network segments of polymer melts are destroyed or disentangled at variable rates. Based on the different choices of macroscopic variation, the single-mode network models can be labeled as stress-dependent and rate-dependent. Phan Thien and Tanner[6] assumed that the rates of creation and loss of network segments were functions of stress, and proposed a nonaffine PTT mode by introducing a slipping coefficient, but the PTT model does not predict the steady shear flow in the wide range of shear rate successfully. Moreover the exponent derived from a single-mode exponential PTT model is $-1$ or so.[1,7] The exponent derived from a single-mode XPP model which is statically unstable is $-4/3$.[7] Tanner and Nasseri[7] proposed a single-mode PTT-XPP model to avoid the very rapid shear thinning of XPP model, but the predicted results are unsatisfactory. Sun et al.[5] expected that a slippage increased with the length of the segments ($Q$), and assumed that

*Correspondence to:* J.-Z. Liang (liangjz@scut.edu.cn).
Contract grant sponsor: NSFC; contract grant number: 51073021.

the slippage depended on $Q^2$ which involves the stress. The model needs seven parameters to predict steady shear viscosity, first normal stress coefficient and extensional viscosity of the mixed dekalin/polybutene oil solvent. Chan Man Fong and De Kee[8] proposed that the rates of creation and loss of segments were the functions of macroscopic deformation rates, their predictions for steady flows which do not include the steady second normal stress using five parameters roughly accords with the experiment results of polymeric solutions. Sun et al.[9] incorporated an internal viscosity idea into the single-mode network model, and proposed two rate-dependent expressions of the shear viscosity and relaxation time, the predicted results about the steady shear viscosity and first normal stress coefficient close to the experimental results using eight parameters.

In addition, there are few other single-mode models using a set of parameters to predict well the steady shear and extensional flows in very wide range of deformation rates. Previously, Giesekus proposed a nonlinear four parameter model, but the exponent derived from this single-mode model is $-1$ or so.[7,10] Souvaliotis and Beris[11] proposed an extended White–Metzner model based on an internal structural parameter, but the model needs different parameter values to predict the steady shear viscosity and first normal stress coefficients. Barnes and Roberts[12] modified White–Metzner equation by introducing the empirical expressions of the shear viscosity and relaxation time, and the modified equation uses six parameters to predict the shear and extensional viscosities, but predicted first and second normal stress coefficients are poor.[13,14]

The steady shear and extensional viscosities, as basic characteristic parameters in polymer processing, can affect processing technology. Moreover the steady first and second normal stress coefficients are also related to the secondary flow, extrudate swell and Weissenberg effect, and so on.[1,15–17] Thus, studying steady viscosities and normal stress coefficients is very important. Meanwhile, further expanding single-mode application scope based on network theory is also necessary and significant. In this article, we analyze the mechanisms of creation and destruction for polymer network junctions and nonaffine movement of network segments, attempt to use a simpler method to present a single-mode model for polymer melts based on the network theory. Furthermore, the effects of model parameters on steady shear and extensional viscosities are discussed. The model predicts simultaneously steady shear viscosity, steady extensional viscosity, and steady first and second normal stress coefficients using four parameters, and predicted results are compared with experimental data from previous literature. In final, the comments on the model are made.

## THEORY AND MODEL

### Basic equations

According to the network theory, the polymeric material is represented by a network of temporary junctions. $\boldsymbol{Q}$ is the end-to-end vector from junction point to junction point. $\Psi(\boldsymbol{Q},t)$, the distribution function, is defined such that $\Psi(\boldsymbol{Q},t)d\boldsymbol{Q}$ is the number of segments per unit volume at time $t$ that have end-to-end vectors between $\boldsymbol{Q}$ and $\boldsymbol{Q}+d\boldsymbol{Q}$. The probability distribution function for network theory obeys a convection equation.[1]

$$\frac{\partial \Psi}{\partial t} = -\left(\frac{\partial}{\partial \boldsymbol{Q}} \cdot [\dot{\boldsymbol{Q}}\,\Psi]\right) + c - l \tag{1}$$

where the dot denotes a derivative with respect to time, the $c$ and $l$ are the rates of creation and loss of network segments, respectively. The rate of junction loss should be equal to the rate of junction creation in the equilibrium state.[18] Hence, the $c$ and $l$ can be written as:

$$c = f\Psi_0, \quad l = f\Psi \tag{2}$$

where $f$ is a rate function of network segments, and $\Psi_0$ is the distribution function at the equilibrium.

Bird et al.[1] have elaborated the relationship between total stress tensor ($\boldsymbol{\pi}$) and the average configuration of polymeric network stands. We also assume that the network stands contribute to $\boldsymbol{\pi}$, and the Hookean stands for network stands are chosen. Thus, the expression of $\boldsymbol{\pi}$ can be written as:

$$\boldsymbol{\pi} = -H\langle \boldsymbol{QQ} \rangle \tag{3}$$

where $H$ is a spring constant.

It can be followed from eq. (3) that

$$(\mathrm{tr}\boldsymbol{\pi}) = -H\langle Q^2 \rangle \tag{4}$$

According to the network model, $\boldsymbol{\pi}$ may be broken up into an isotropic portion which is present even at equilibrium, and a nonisotropic portion which is stress tensor ($\boldsymbol{\tau}$). So $\boldsymbol{\pi}$ can be written as the sum of two parts:[1]

$$\boldsymbol{\pi} = -nKT\boldsymbol{\delta} + \boldsymbol{\tau} \tag{5}$$

where $n$ is the number density of network segments, $K$ is the Boltzmann constant, $T$ is the absolute temperature, $\boldsymbol{\delta}$ is an unit tensor. At the equilibrium, the stress tensor is zero. Substituting eq. (3) into eq. (5), the following expression can be deduced.

$$H\langle \boldsymbol{QQ} \rangle_0 = nKT\boldsymbol{\delta} \tag{6}$$

### Analysis

In general, the rates of creation and loss for network segments play an important role in the viscoelastic behavior.[1,5,8] As stated above, many different expressions of the creation and loss for network segments have been proposed to capture the viscoelastic behavior of polymer melts. Some researchers[5–7] assumed that the rates of creation and loss for network segments were the functions of the stress. Furthermore, many researchers[8,9,12,19] considered that these rates were the functions of macroscopic deformation rates. Therefore, based on previous reports we assume that the creation and destruction of network junctions depend on the stress ($\tau$) and the rate parameter ($\dot{\gamma}_0$). Meanwhile, we also note that the shear viscosity ($\eta_s$) is determined by the stress and rate. Thus, we propose that rates of creation and loss are appropriately written as:

$$f = [g(1 + \dot{\gamma}_0^a)]/\eta_s \tag{7}$$

where $a$ is a shear thinning parameter, $g$ is a parameter of relaxation modulus. The rate parameter is non dimensional to eliminate an unconformity of units, and the value of $\dot{\gamma}_0$ is equal to the value of shear rate ($\dot{\gamma}$) in steady shear flow, the value of $\dot{\gamma}_0$ is equal to the value of extensional rate ($\dot{\varepsilon}$) in steady extensional flow.

In fact, a test strand of polymer network is subjected to some complex forces in the polymeric flow. The externally applied force stretches the test strand, meanwhile, the intrastand force resists stretching of the stand. Other important forces, such as those resulting from chain–chain interactions, may be nonlocal and can be transmitted over large distances compared with the test strand.[20] When the test strand is extended, the nearby, interconnected strands are also extended. The backbone forces of these nearby and interconnected extended strands intensify the motion which may shorten the test strand.[20] With the increases of $Q$ and deformation rates, the restoring force, which shortens the test strand, will increase. Therefore, we regard polymer backbone as the investigating object, and assume that the end-to-end distance of the segment is much less than its maximum length ($Q_0$), and use a partially shortening form to describe the nonaffine motion of network segments as follows:

$$\dot{\boldsymbol{Q}} = \mathbf{k} \cdot \boldsymbol{Q} - \frac{Q^2}{Q_0^2} \cdot \dot{\boldsymbol{\gamma}} \cdot \boldsymbol{Q} \tag{8}$$

where $\mathbf{k}$ is the velocity gradient tensor, and $\dot{\boldsymbol{\gamma}} = \mathbf{k} + \mathbf{k}^{\mathrm{T}}$ is the rate of deformation tensor, and $\mathbf{k}^{\mathrm{T}}$ is the transpose of velocity gradient tensor. The parameter $Q_0$, a statistical average value, is a ratio of the maximum length sum of backbone segments including linking branched segments to monomer numbers of backbone. Because the ratio of extensional viscosity to shear viscosity is three when deformation rates close to zero,[1] it may be assumed reasonably that the value of $Q_0$ in steady extensional flow is three times larger than the value in steady shear flow.

Substituting eqs. (2)–(4), (6), and (8) into eq. (1), multiplying the expression by $\boldsymbol{QQ}$, and integrating over the configuration space, we produce a convection equation.

$$\frac{d}{dt}\langle \boldsymbol{QQ} \rangle = \mathbf{k} : \left\langle \boldsymbol{Q} \frac{\partial}{\partial \boldsymbol{Q}} \cdot \boldsymbol{QQ} \right\rangle - \dot{\boldsymbol{\gamma}} : \left\langle \frac{Q^2}{Q_0^2} \boldsymbol{Q} \frac{\partial}{\partial \boldsymbol{Q}} \cdot \boldsymbol{QQ} \right\rangle + f(\langle \boldsymbol{QQ} \rangle_0 - \langle \boldsymbol{QQ} \rangle) \tag{9}$$

where $\langle \cdots \rangle$ indicates the average taken over the configuration space of the network stands. Substituting eq. (7) into eq. (9) and applying Peterlin analysis, we finally arrive at a constitutive equation for polymer melts as follows:

$$g\boldsymbol{\tau}(1 + \dot{\gamma}_0^a) + \eta_s \boldsymbol{\tau}_{(1)} - \frac{[\eta_s^2 (tr\boldsymbol{\tau}) - 3g\tilde{\eta}\eta_s(1 + \dot{\gamma}_0^a)](\dot{\boldsymbol{\gamma}} \cdot \boldsymbol{\tau} + \boldsymbol{\tau} \cdot \dot{\boldsymbol{\gamma}})}{bg\tilde{\eta}(1 + \dot{\gamma}_0^a)} = -[g\tilde{\eta}(1 + \dot{\gamma}_0^a) + \frac{2\eta_s (tr\boldsymbol{\tau}) - 6g\tilde{\eta}(1 + \dot{\gamma}_0^a)}{b}] \dot{\boldsymbol{\gamma}} \tag{10}$$

where $\tilde{\eta} = nKT\lambda$, $b$ is an extensibility parameter for the segments given by $b = HQ_0^2/KT$, $\boldsymbol{\tau}_{(1)}$ is the upper convected derivative of $\boldsymbol{\tau}$ and is given by:

$$\boldsymbol{\tau}_{(1)} = (D\boldsymbol{\tau}/Dt) - \mathbf{k} \cdot \boldsymbol{\tau} - \boldsymbol{\tau} \cdot \mathbf{k}^{\mathrm{T}} \tag{11}$$

where $D/Dt$ is the material derivative.

## EXPERIMENTAL DATA

To examine predictive ability of this model objectively, the experimental data are adopted as follows: Pivokonsky et al.[21] conducted the rheology of two highly branched low density polyethylene (LDPE) materials (LDPE Bralen, Slovnaft, Slovakia and LDPE Escorene, Exxon, USA). For two kinds of LDPE, the steady shear viscosity and first normal stress coefficient at low shear rate were measured with the advanced rheometric expansion system (ARES 2000, Rheometrics), the steady shear viscosity and first normal stress coefficient at high shear rate were obtained with the capillary rheometer RH7 (Rosand Precision). The uniaxial extensional viscosity was measured using the ARES 2000 rheometer equipped with the SER universal testing platform (SER-HV-A01 model). The experiment was performed at 200°C. The

**TABLE I**
**The Basic Characteristics of Two LDPE melts at 200°C**

| Material | $M_w$ (g mol$^{-1}$) | $M_w/M_n$ | $\eta_0$ (Pa s) |
|---|---|---|---|
| LDPE Bralen | 262,000 | 8.19 | 62,319 |
| LDPE Escorene | 366,300 | 12.1 | 77,103 |

Where $M_w$ is weight average molar mass, $M_w/M_n$ is polydispersity coefficient.

molecular characteristics of two materials at 200°C are presented in Table I.[21,22] For detailed descriptions of the experiment, see Pivokonsky et al.[21]

## RESULTS AND DISCUSSION

### Equations of steady shear flow

The velocity components for steady shear flow are:

$$v_1 = \dot{\gamma}\, x_2, \quad v_2 = 0, \quad v_3 = 0 \tag{12}$$

where $v$ is velocity. The stress relevant equations can be written as:

$$g\tau_{11}(1+\dot{\gamma}^a) - 2\eta_s\tau_{12}\,\dot{\gamma} - \frac{2\tau_{12}\,\dot{\gamma}[\eta_s^2(tr\tau) - 3g\tilde{\eta}\eta_s(1+\dot{\gamma}^a)]}{bg\tilde{\eta}(1+\dot{\gamma}^a)} = 0 \tag{13}$$

$$g\tau_{22}(1+\dot{\gamma}^a) - \frac{2\tau_{12}\,\dot{\gamma}[\eta_s^2(tr\tau) - 3g\tilde{\eta}\eta_s(1+\dot{\gamma}^a)]}{bg\tilde{\eta}(1+\dot{\gamma}^a)} = 0 \tag{14}$$

$$g\tau_{12}(1+\dot{\gamma}^a) - \eta_s\tau_{22}\,\dot{\gamma} - \frac{\dot{\gamma}(\tau_{11}+\tau_{22})[\eta_s^2(tr\tau) - 3g\tilde{\eta}\eta_s(1+\dot{\gamma}^a)]}{bg\tilde{\eta}(1+\dot{\gamma}^a)} = -\dot{\gamma}\left[g\tilde{\eta}(1+\dot{\gamma}^a) + \frac{2\eta_s(tr\tau) - 6g\tilde{\eta}(1+\dot{\gamma}^a)}{b}\right] \tag{15}$$

$$\tau_{13} = \tau_{23} = \tau_{33} = 0 \tag{16}$$

The shear viscosity is given by:

$$\eta_s = -\tau_{12}\big/\dot{\gamma} \tag{17}$$

Combining eqs. (13)–(17) generates an equation in $\eta_s$ which can be written by:

$$16\dot{\gamma}^6\eta_s^9 + 16g^2\dot{\gamma}^4(1+\dot{\gamma}^a)^2\eta_s^7 + 8bg^2\tilde{\eta}\dot{\gamma}^4(1+\dot{\gamma}^a)^2\eta_s^6 + 8bg^4\tilde{\eta}\dot{\gamma}^2(1+\dot{\gamma}^a)^4\eta_s^4 + 4g^4\tilde{\eta}^2\dot{\gamma}^2(2b-3)(1+\dot{\gamma}^a)^4\eta_s^3 + b^2g^6\tilde{\eta}^2(1+\dot{\gamma}^a)^6\eta_s + bg^6\tilde{\eta}^3(6-b)(1+\dot{\gamma}^a)^6 = 0 \tag{18}$$

The first and second normal stress coefficients are respectively given by:

$$\Psi_1 = (\tau_{22}-\tau_{11})\big/\dot{\gamma}^2 = 2\eta_s^2\big/[g(1+\dot{\gamma}^a)] \tag{19}$$

$$\Psi_2 = (\tau_{33}-\tau_{22})\big/\dot{\gamma}^2 = -[4\eta_s^5\dot{\gamma}^2 + 6g^2\tilde{\eta}\eta_s^2(1+\dot{\gamma}^a)^2]\big/[bg^3\tilde{\eta}(1+\dot{\gamma}^a)^3 + 4g\eta_s^3\dot{\gamma}^2(1+\dot{\gamma}^a)] \tag{20}$$

### Equations of steady uniaxial extensional flow

The velocity field of steady uniaxial extensional flow can be written as:

$$v_1 = -\dot{\varepsilon}\, x_1\big/2, \quad v_2 = -\dot{\varepsilon}\, x_2\big/2, \quad v_3 = \dot{\varepsilon}\, x_3 \tag{21}$$

Substituting eq. (21) into eq. (10) yields some equations as follows:

$$g\tau_{11}(1+\dot{\varepsilon}^a) + \eta_s\tau_{11}\,\dot{\varepsilon} + \frac{2\tau_{11}\,\dot{\varepsilon}[\eta_s^2(tr\tau) - 3g\tilde{\eta}\eta_s(1+\dot{\varepsilon}^a)]}{bg\tilde{\eta}(1+\dot{\varepsilon}^a)} = \dot{\varepsilon}\left[g\tilde{\eta}(1+\dot{\varepsilon}^a) + \frac{2\eta_s(tr\tau) - 6g\tilde{\eta}(1+\dot{\varepsilon}^a)}{b}\right] \tag{22}$$

$$g\tau_{22}(1+\dot{\varepsilon}^a) + \eta_s\tau_{22}\,\dot{\varepsilon} + \frac{2\tau_{22}\,\dot{\varepsilon}[\eta_s^2(tr\tau) - 3g\tilde{\eta}\eta_s(1+\dot{\varepsilon}^a)]}{bg\tilde{\eta}(1+\dot{\varepsilon}^a)} = \dot{\varepsilon}\left[g\tilde{\eta}(1+\dot{\varepsilon}^a) + \frac{2\eta_s(tr\tau) - 6g\tilde{\eta}(1+\dot{\varepsilon}^a)}{b}\right] \tag{23}$$

$$g\tau_{33}(1+\dot{\varepsilon}^a) - 2\eta_s\tau_{33}\,\dot{\varepsilon} - \frac{4\tau_{33}\,\dot{\varepsilon}[\eta_s^2(tr\tau) - 3g\tilde{\eta}\eta_s(1+\dot{\varepsilon}^a)]}{bg\tilde{\eta}(1+\dot{\varepsilon}^a)} = -2\,\dot{\varepsilon}\left[g\tilde{\eta}(1+\dot{\varepsilon}^a) + \frac{2\eta_s(tr\tau) - 6g\tilde{\eta}(1+\dot{\varepsilon}^a)}{b}\right] \tag{24}$$

The uniaxial extensional viscosity is defined by:

$$\eta_e = (\tau_{11}-\tau_{33})\big/\dot{\varepsilon} \tag{25}$$

Combining eqs. (22)–(25) generates a cubic equation of $\eta_e$ which can be written as:

$$16\eta_s^4\dot{\varepsilon}^4\eta_e^3 + [8bg^2\tilde{\eta}\eta_s^2\dot{\varepsilon}^2(1+\dot{\varepsilon}^a)^2 + 4(6-b)g\tilde{\eta}\eta_s^3\dot{\varepsilon}^3(1+\dot{\varepsilon}^a)]\eta_e^2 + [6bg^3\tilde{\eta}^2\eta_s\,\dot{\varepsilon}(1+\dot{\varepsilon}^a)^3 - b^2g^3\tilde{\eta}^2\eta_s\,\dot{\varepsilon}(1+\dot{\varepsilon}^a)^3 + 2bg^2\tilde{\eta}^2\eta_s^2\dot{\varepsilon}^2(6-b)(1+\dot{\varepsilon}^a)^2 + b^2g^4\tilde{\eta}^2(1+\dot{\varepsilon}^a)^4]\eta_e + 3bg^4\tilde{\eta}^3(6-b)(1+\dot{\varepsilon}^a)^4 = 0 \tag{26}$$

### Dependences of steady shear and extensional viscosities on model parameters

When deformation rates close to zero, the zero-shear viscosity ($\eta_0$) is $(b-6)\tilde{\eta}\big/b$ derived from eq. (18),

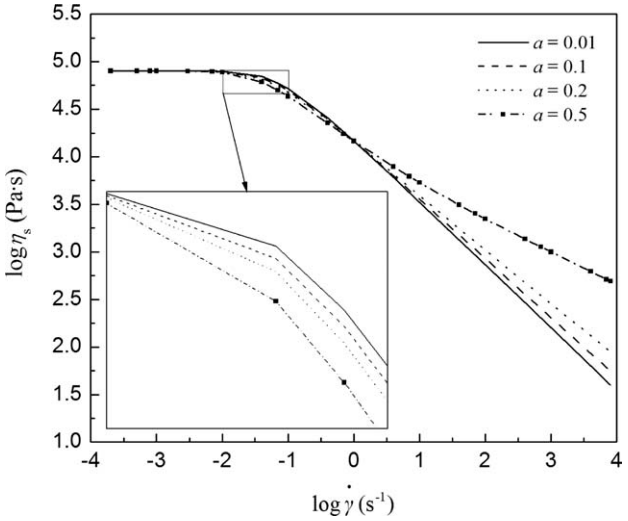


**Figure 1** Dependence of $\eta_s$ on $a$.

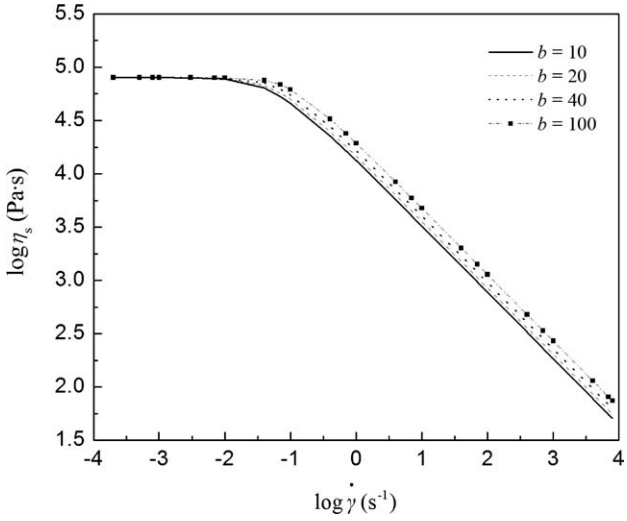


**Figure 3** Dependence of $\eta_s$ on $b$.

and the steady extensional viscosity is $3\eta_0$ derived from eq. (26), which also agrees with the experimental facts.[1,23,24] The parameters $a$, $b$, and $g$ play an important role in this model. Based on eqs. (18) and (26) simple simulations about $a$, $b$, and $g$ are carried out to study the dependences of $\eta_s$ and $\eta_e$ on one parameter by fixing other parameters. The basic parameters used are as follows: $\eta_0$ is 80000 Pa $s^{-1}$, $a$ is 0.1, $b$ is 20, $g$ is 3000 Pa. Figures 1 and 2 shows the dependences of $\eta_s$ and $\eta_e$ on $a$, respectively. It can be seen from Figures 1 and 2 that when $\dot{\gamma}$ is less than 1 $s^{-1}$, $\eta_s$ reduces approximately with an increasing $a$, with the further increase of $\dot{\gamma}$, $\eta_s$ increases with the increasing $a$, and $\eta_e$ increases approximately with the increasing $a$ at fixed $\dot{\varepsilon}$. So the parameter $a$ plays an adjust effect, and can avoid the rapid reductions of $\eta_s$ and $\eta_e$ at high deformation rates.

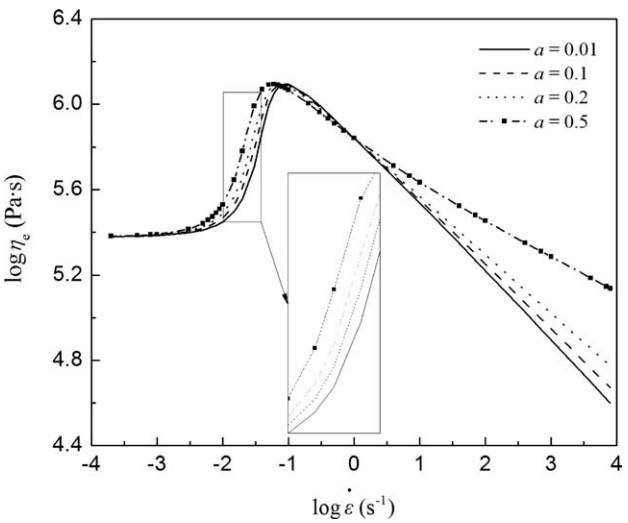


**Figure 2** Dependence of $\eta_e$ on $a$.

Figures 3 and 4 show the dependences of $\eta_s$ and $\eta_e$ on $b$, respectively. It can be seen from Figure 3 that $\eta_s$ increases with an increase of $b$. Because the $b$ is proportional to the $Q_0$, at the same shear rate an increasing $Q_0$ weakens the chain shortening, leading to the stress increase, the shear viscosity increases accordingly. According to eq. (18), as $b$ tends to infinity, this shorten effect may be neglected, $\eta_s$ is a constant, which also accords with the basic network model.[1] It can also be seen from the Figure 4 that with the increase of $b$ the strain hardening extent enhances at the same extensional rate. This can be explained that with the increasing extensional rate the extensional viscosity also increases for polymer melts occurring with strain hardening phenomenon, and extensional strength improves, which contributes to further melt extension, the value of $b$ also increases. On the other hand, owing to a contribution of branched chains, the branched polymer has large value of $b$ compared with the linear polymer. The higher the branched degree, the larger is the value of $b$, so the strain hardening extent enhances. This predicted behavior also closes to the experimental facts,[23,24] and the dependences of $\eta_s$ and $\eta_e$ on $b$ based on our model accords to some simulations based on POM, XPP, PTT-XPP model.[7,25,26] Figures 5 and 6 show the dependences of $\eta_s$ and $\eta_e$ on $g$, respectively. It can be seen from Figures 5 and 6 that $\eta_s$ increases with an increase of $g$, and the deformation rates occurring with shear thinning or strain hardening phenomena increases. Because the $g$ reflects an ability of resist deformation, the resistance to deformations enhances with the increase of $g$. Therefore, the shear viscosity increases, moreover the shear thinning and strain hardening phenomena appear at relatively high deformation rates.

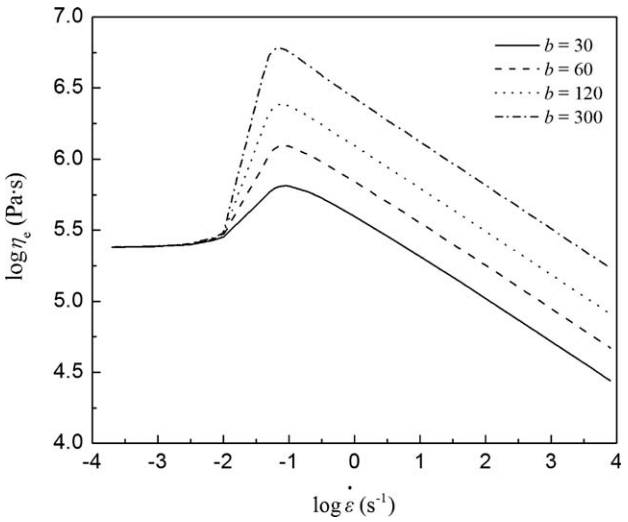


**Figure 4** Dependence of $\eta_e$ on $b$.

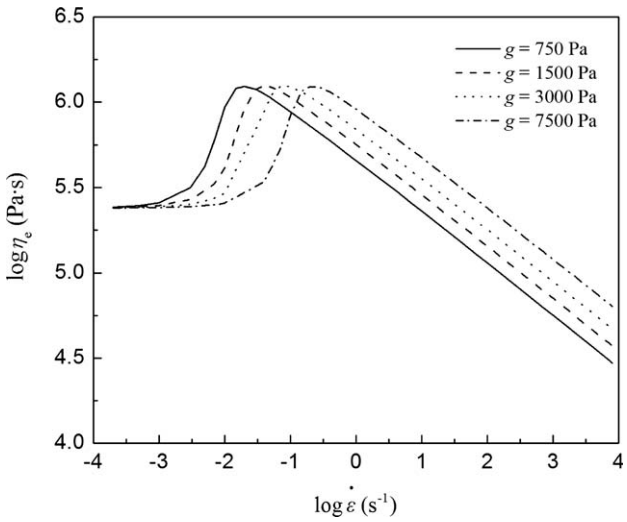


**Figure 6** Dependence of $\eta_e$ on $g$.

### Experimental verification

In the model, we have defined four parameters, $\eta_0$, $a$, $b$, and $g$ to describe the steady shear and extensional flows. The parameter $\eta_0$ is determined by referring the literature.[21,22] The structural parameters are difficult to be obtained from experiments directly for many models,[2,5–13,19,21,22,25,26] so the values of $a$, $b$, and $g$, are got by fitting experimental data of $\eta_s$. Considering the experimental data of Pivokonsky et al.[21] LDPE Bralen is produced in an autoclave way resulting in more globular structures. Moreover, it has higher strain hardening capability than LDPE Escorene,[22] LDPE Bralen can also store more elastic strain energy than LDPE Escorene due to a relatively smaller size of the polymer coil or enhanced chain stretching.[27] It can be seen from Table I that two kinds of LDPE have different molecular weights and polydispersity coefficients. Compared with LDPE Bralen, LDPE Escorene has high molecular weight and zero-shear viscosity, so it can be deduced that LDPE Escorene should undergo longer relaxation process than LDPE Bralen under the same processing conditions. Moreover, $b$ also represents the maximum extensibility energy which can be stored in the polymeric materials for nonlinear deformations of the segments. The $g$ reflects an ability of resist deformation. Based on the above analysis, the model predictions using $b = 34$, $g = 4300$ Pa for LDPE Bralen and $b = 19$, $g = 3200$ Pa for LDPE Escorene can give a good agreement with experimental data of $\eta_s$. Meanwhile, we use $a = 0.05$ for LDPE Bralen and $a = 0.08$ for LDPE Escorene to describe the shear thinning phenomenon well.

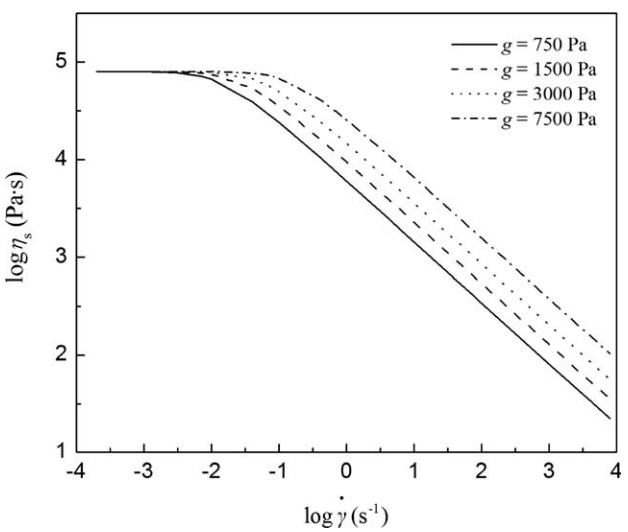


**Figure 5** Dependence of $\eta_s$ on $g$.

Predicted $\eta_s$, $\Psi_1$, and $\Psi_2$ calculated from eqs. (18)–(20) are compared with experimental data. The comparisons between measured data and the predictions of the model for the LDPE Bralen are represented in the Figures 7 and 8, it can be found that the model has a good capability to predict $\eta_s$ for the LDPE Escorene with optimal parameters, and predicted $\Psi_1$ and $\Psi_2$ of the model close to the experimental data. Similarly, the predictions of $\eta_s$, $\Psi_1$, and $\Psi_2$ also close to the experiment facts for the LDPE Escorene as shown in Figures 9 and 10. Following the assumption of eq. (7), we get $\eta_s$ from eq. (18), and then obtain $\eta_e$ from eq. (26) based on the parameter values which are also used in the steady shear flow. Figures 8 and 10 also depict the comparisons between measured uniaxial extensional viscosity data and the model predictions for the LDPE Bralen and the LDPE Escorene, respectively. As shown in the predictions and experiments, in a bilogarithm coordinate system $\eta_e$ is initially an increasing function of $\dot{\varepsilon}$, it reaches a maximum and then reduces with further increase in $\dot{\varepsilon}$. When $\dot{\varepsilon}$ is closed to 0.1 $s^{-1}$ for the LDPE Escorene, $\eta_e$ reaches a

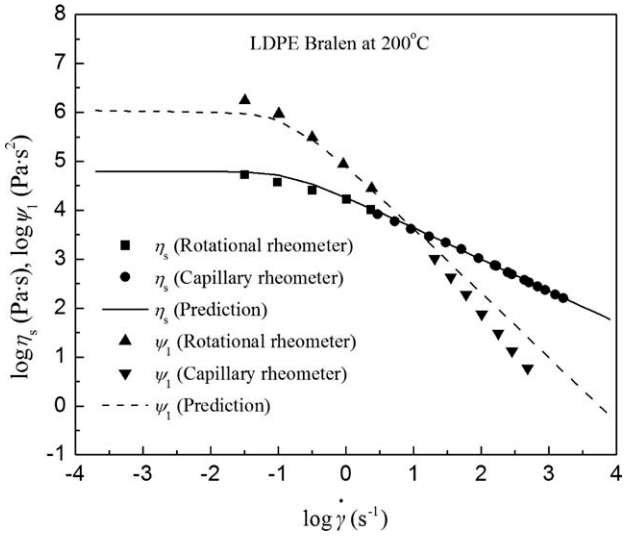


**Figure 7** Comparison between measured shear viscosity and first normal stress coefficient data from LDPE Bralen at 200°C and the predictions.

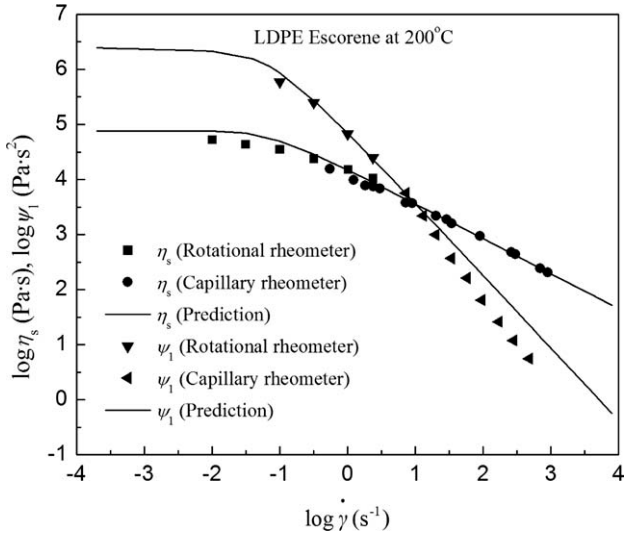


**Figure 9** Comparison between measured shear viscosity and first normal stress coefficient data from LDPE Escorene at 200°C and the predictions.

maximum, and when $\dot{\varepsilon}$ increases to 0.3 s$^{-1}$ or so for the LDPE Bralen, $\eta_e$ also reaches a maximum. This illustrates this model can predict when a strain hardening phenomenon happens, and predicted $\eta_e$ is also closed to the experimental data.

## DISCUSSION

It cannot be denied that the physical significance is relatively simple for this single-mode model. However, the analytical forms of $\eta_s$, $\Psi_1$, and $\Psi_2$, and $\eta_e$ are easily obtained based on this single-mode model without a complex statistical simulation, the steady shear and extensional properties are simultaneously predicted using four parameters determined by steady shear viscosity. Even if $a$ is zero and the values of $b$, $g$, and $\eta_0$ are arbitrary in the model, the power law derived from eq. (18) is $\eta_s \sim \dot{\gamma}^{-2/3}$ at high shear rate, which also closes to experimental facts of polymer melts.[17,21,28–30] Because the data of steady shear viscosity is easy to be obtained from the experiments, the parameters of this model are easy to be determined. Furthermore the secondary flow and extrudate swell are related to normal stress coefficients.[1,15–17] Considering the good predictions, the model is also convenient to use together with finite element software for simulating these phenomena of polymer melts.

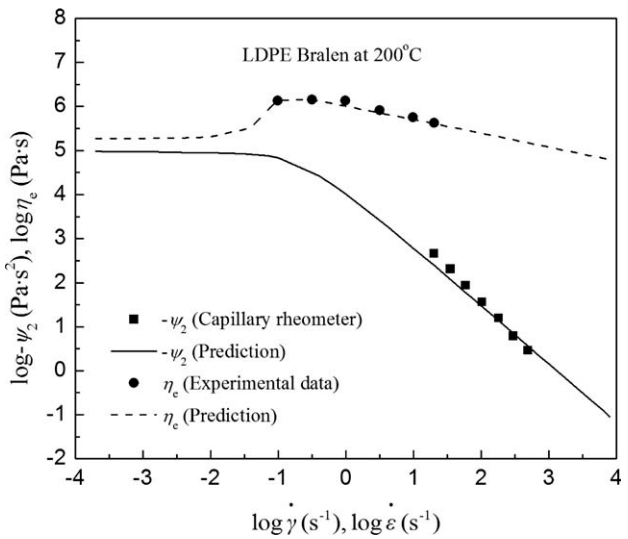


**Figure 8** Comparison between measured second normal stress coefficient and uniaxial extensional viscosity data from LDPE Bralen at 200°C and the predictions.

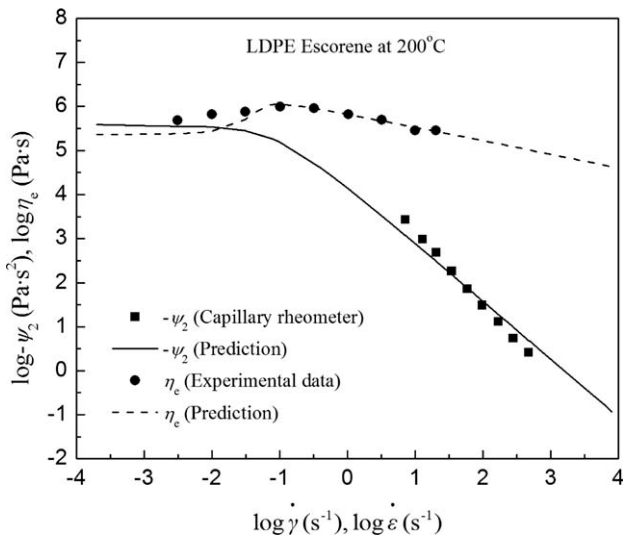


**Figure 10** Comparison between measured second normal stress coefficient and uniaxial extensional viscosity data from LDPE Escorene at 200°C and the predictions.

## CONCLUSIONS

In this article, we propose a stress- and rate-dependent function to describe creation and destruction of polymer junctions. Moreover, we also introduce a movement expression to describe nonaffine movement of network junctions. Based on the network theory a single-mode model of polymer melts is derived in the shear and extensional flows, and the equations of $\eta_s$, $\Psi_1$, and $\Psi_2$, and $\eta_e$ are derived from the model accordingly. Furthermore, the dependences of $\eta_s$ and $\eta_e$ on model parameters are also discussed for the model. Without the complex statistical simulation, the model with four parameters has good predictive and fitting capabilities of steady shear and extensional flows for two low density polyethylene melts at 200°C reported from previous literature in very wide range of deformation rates. Compared with other single-mode rheological models, predicted shear thinning behavior for this model also closes to experimental facts without regard to the parameter values.

### References


1. Bird, R. B.; Curtiss, C. F.; Armstrong, R. C.; Hassager, O. Dynamics of Polymeric Liquids: Kinetic Theory; Wiley: New York, 1987; Vol.2.
2. Liang, J. Z.; Zhong, L. Polym Eng Sci 2010, 50, 2190.
3. Qu, J. P.; Wei, B. H.; Yang, Z. T.; Cai, Y. H. J Appl Polym Sci 2009, 113, 1560.
4. Liang, J. Z. Polym Plast Technol Eng 2007, 46, 475.
5. Sun, N.; Chan Man Fong, C.; De Kee, D. Rheol Acta 2000, 39, 174,.
6. Thien, N. P.; Tanner, R. I. J Non-Newtonian Fluid Mech 1977, 2, 353.
7. Tanner, R. I.; Nasseri, S. J Non-Newtonian Fluid Mech 2003, 116, 1,.
8. Chan Man Fong, C.; De Kee, D. Phys A Stat Theor Phys 1995, 218, 56.
9. Sun, N.; Chan Man Fong, C.; De Kee, D. J Non-Newtonian Fluid Mech 2000, 95, 135,.
10. Gauri, V.; Koelling, K. W. Rheol Acta 1997, 36, 555.
11. Souvaliotis, A.; Beris, A. J Rheol 1992, 36, 241.
12. Barnes, H.; Roberts, G. J Non-Newtonian Fluid Mech 1992, 44, 113.
13. Zatloukal, M. J Non-newtonian Fluid Mech 2003, 113, 209.
14. Larson, R. G. Constitutive Equations for Polymer Melts and Solutions; Butterworths: Boston, 1988.
15. Liang, J. Z. Plast Rubber Compos Process Appl 1993, 19, 311.
16. Liang, J. Z.; Li, R. K. Y. J Appl Polym Sci 1999, 73, 1451.
17. Liang, J. Z. Polym Int 2002, 51, 1473.
18. Petruccione, F. Continuum Mech Thermodyn 1989, 1, 97.
19. Chan Man Fong, C.; De Kee, D. J Non-Newtonian Fluid Mech 1995, 57, 39.
20. Wedgewood, L. E.; Geurts, K. R. Rheol Acta 1995, 34, 196.
21. Pivokonsky, R.; Zatloukal, M.; Filip, P. J Non-Newtonian Fluid Mech 2006, 135, 58.
22. Rolón-Garrido, V. H.; Pivokonsky, R.; Filip, P.; Zatloukal, M.; Wagner, M. H. Rheol Acta 2009, 48, 691.
23. Baird, D. G.; Collias, D. I. Polymer Processing: Principles and Design; Wiley: New York, 1998.
24. Zhou, C. X. Polymer Rheological Experiment and Application; Shanghai Jiao Tong University Press: Shanghai, 2003.
25. Blackwell, R.; McLeish, T.; Harlen, O. J Rheol 2000, 44, 121.
26. Aguayo, J.; Tamaddon-Jahromi, H.; Webster, M. J Non-Newtonian Fluid Mech 2006, 134, 105.
27. Rolón-Garrido, V. H.; Wagner, M. H. Rheol Acta 2007, 46, 583.
28. Liang, J. Z. Macromol Mater Eng 2001, 286, 714.
29. Liang, J. Z.; Yang, J.; Tang, C. Y. J Appl Polym Sci 2011, 119, 1835.
30. Yang, J.; Liang, J. Z.; Tang, C. Y. Polym Test 2009, 28, 907.